Int. J. Solids Structures, 1967, Vol. 3, pp. 97 to 115. Pergamon Press Ltd. Printed in Great Britain

INITIAL POST-BUCKLING BEHAVIOR OF TOROIDAL SHELL SEGMENTS*

JOHN W. HUTCHINSON

Harvard University, Cambridge, Massachusetts

Abstract—The initial post-buckling behavior of double curvature shell segments subject to several loading conditions is determined on the basis of Koiter's general theory of initial post-buckling behavior. Previously, the classical buckling loads associated with these shells were shown to be strongly dependent on the two radii of curvature and their relative magnitudes. Here, the initial post-buckling behavior and associated imperfection-sensitivity are also seen to be strongly dependent on the two curvatures.

INTRODUCTION

AMONG those structures whose buckling strengths are known to be highly sensitive to structural imperfections are spherical and cylindrical shells subject to external pressure, axially loaded narrow cylindrical panels, some simple trusses and, of course, the axially compressed cylindrical shell. The classical (linear) buckling analysis of such a structure, by itself, is incapable of predicting the buckling strength. Accurate predictions for a given structure require exact knowledge of the initial imperfections of the unloaded structure; but, in general, such information is not at the disposal of either the analyst or designer. To date, mainly because of the difficulty of measuring imperfections of actual as well as test specimens, analytic work has served to provide information as to the relative imperfection-sensitivity of structures and, thus, to qualitatively establish the validity or non-validity of the classical buckling analysis.

In this paper some double curvature shell structures, whose classical buckling behavior has only recently been studied, are investigated with the view toward determining their initial post-buckling behavior and, what is closely related, the dependence of their buckling strengths on imperfections in the form of initial deviations of the shell middle surface from the perfect configuration. This study is made within the framework of Koiter's general theory of initial post-buckling behavior [1].

The shell segments shown in Fig. 1 can be thought of as sections of complete toroidal shells. The classical buckling analysis of these shells has been given by Stein and McElman [2] for three different pressure loadings. Results of their analysis for the case of buckling under lateral pressure are reproduced in Fig. 2. Here, the buckling parameter, $K = pr_y l^2/\pi^2 D$ (where p is the lateral pressure, $D = Eh^3/12(1-\nu^2)$ is the bending stiffness, h is the shell thickness and ν is Poisson's ratio) is a function of the length parameter

$$z = \sqrt{(1-\nu^2)}l^2/r_y h$$

and the ratio of the two radii of curvatures r_y/r_x. An elucidation of further details relevant

* This work was supported in part by the National Aeronautics and Space Administration under Grant NsG-559, and by the Division of Engineering and Applied Physics, Harvard University.

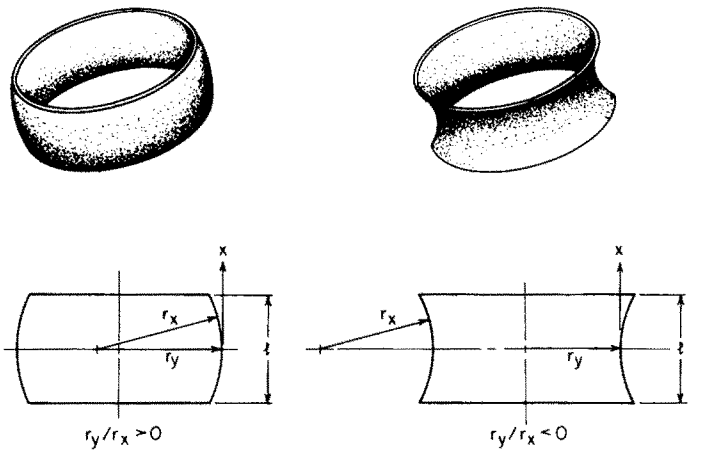

FIG. 1. Configuration of toroidal segments.

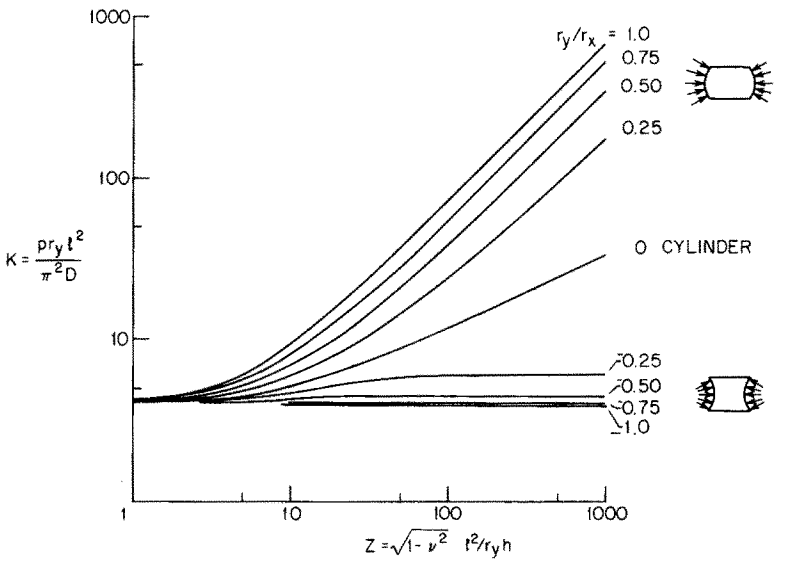

FIG. 2. Classical buckling of toroidal segments under lateral pressure.

to this plot, such as boundary conditions, will be given in the next section. At this point, however, attention is drawn to the significant difference between the predicted buckling strengths of the bowed-out and the bowed-in shells which are otherwise of essentially the same dimensions. On the basis of the classical buckling analysis the buckling strength of the bowed-out shell can be several orders of magnitude larger than that of the bowed-in configuration. One might conjecture, and, indeed, this will prove to be the case, that the initial post-buckling analysis indicates a significantly increased imperfection-sensitivity hand-in-hand with the higher classical buckling strength.

Two other loading conditions are studied in addition to the lateral pressure case. Quite similar, yet more imperfection-sensitive, is the external pressure case. In the third

case the classical and initial post-buckling behavior of the bowed-out segments subject to axial tension is determined.

CLASSICAL BUCKLING ANALYSIS

Here a brief exposition of Stein and McElman's classical analysis is given. Buckling under axial tension, although not considered by these authors, is also included in the results given below. Donnell-type nonlinear shell theory is employed in the classical, as well as the initial post-buckling, analysis of the toroidal segments. Consideration is restricted to segments which are shallow with respect to the axial coordinate, that is $l/r_x \ll 1$. The linear Donnell buckling equations, given by Stein and McElman, are written here in terms of the normal displacement w and a stress function f

$$D\nabla^4 w+\frac{1}{r_y}f_{,xx}+\frac{1}{r_x}f_{,yy}-\lambda N_x^0 w_{,xx}-\lambda N_y^0 w_{,yy}=0 \tag{1}$$

and

$$\frac{1}{Eh}\nabla^4 f-\frac{1}{r_y}w_{,xx}-\frac{1}{r_x}w_{,yy}=0 \tag{2}$$

where E is Young's Modulus and the assumption of shallowness in the axial direction permits us to write $\nabla^4=(_{,xx}+_{,yy})^2$. The additional buckling membrane stresses are given by $N_x=f_{,yy}$, $N_y=f_{,xx}$ and $N_{xy}=-f_{,xy}$.

In equation (1) λN_x^0 and λN_y^0 represent the x and y components of the resultant membrane stresses associated with the prebuckling deformation of the perfect shell. Except for a narrow region near each end of the shell the prebuckling state of stress is homogeneous and, for each loading system investigated here, is linearly dependent on the externally applied load. In this paper the edge distortions are neglected and, thus, the membrane stresses λN_x^0 and λN_y^0 are constant over the entire shell. The load parameter λ is linearly related to the applied load and N_x^0 and N_y^0 are assumed to be fixed in some definite manner depending on the particular loading system. Refined analyses for cylindrical shells [3] accounting for the end distortions have shown that, except for very short shells, the local end effects can be neglected when the buckle pattern has only one half wavelength over the axial length. It is expected that approximate calculations neglecting the edge zone distortions should not introduce significant errors as long as $z > 10$ say. Since the underlying aim of this study is to discover the role of the two radii of curvature, r_x and r_y, in determining the initial post-buckling behavior, we follow Stein and McElman and choose the boundary conditions which are most tractable from the point of view of the analysis. At each end of the shell the normal and circumferential tangential displacements are required to vanish as is the additional buckling stress $N_x=f_{,yy}$ and the additional bending stress M_x. In terms of w and f these are equivalent to

$$w=w_{,xx}=f_{,xx}=f=0 \quad \text{at} \quad x=0,l. \tag{3}$$

Other boundary conditions, completely clamped for example, can be expected to give quite different predictions for the classical buckling load. Nevertheless, it is felt that a complete study based on these boundary conditions should lend at least qualitative insight to the imperfection-sensitivity of similar shells with other edge conditons.

Equations (1) and (2) with the boundary conditions (3) comprise the linear eigenvalue problem for determining the classical buckling load. The eigenfunction

$$w_{mn} = \sin\frac{m\pi x}{l}\sin\frac{ny}{r_y}$$

$$f_{mn} = -\frac{Ehl^2}{\pi^2 r_y}\left[\frac{m^2+\bar{n}^2 r_y/r_x}{(m^2+\bar{n}^2)^2}\right]\sin\frac{m\pi x}{l}\sin\frac{ny}{r_y}$$

is associated with the eigenvalue

$$\lambda_{mn} = -\frac{D\pi^2}{l^2}\frac{1}{(N_x^0 m^2 + N_y^0\bar{n}^2)}\left[(m^2+\bar{n}^2)^2 + \frac{12z^2}{\pi^4}\frac{(m^2+\bar{n}^2 r_y/r_x)^2}{(m^2+\bar{n}^2)^2}\right]$$

where $\bar{n} = nl/\pi r_y$. The classical buckling load λ_c corresponds to the minimum value of λ_{mn} among all possible integer values of m and n. For each of the three loading conditions considered in this paper the minimum value of λ_{mn} always occurs for $m = 1$. The minimum with respect to n is found by treating $\bar{n}$ as a continuous variable under the assumption, to be verified *a posteriori*, that n is sufficiently large. The restriction to $n > 5$, say, is necessary in any case since Donnell-type equations are being used.

The indicated calculations were carried out with the aid of a digital computer and will be presented in sections to follow. For the two pressure loadings the results are in agreement with Stein and McElman's calculations.

DESCRIPTION OF INITIAL POST-BUCKLING ANALYSIS

The linear buckling analysis predicts the critical load and associated buckling mode, or modes, of the structure. A *unique buckling mode* is predicted in every case considered in this paper. The initial post-buckling analysis of such a structure provides a single nonlinear, algebraic equation of equilibrium relating the applied load to the deflection in the buckling mode. The magnitude of the initial imperfection also appears in this equation.

The normal displacement of the buckling mode deflection is

$$w = \xi h \sin(\pi x/l)\sin(ny/r_y) \tag{4}$$

where n is determined by the classical analysis and ξ is the mode deflection relative to the shell thickness h. Initial imperfections in the form of the buckling modes are most critical if, indeed, imperfections play any degrading role at all. In the present analysis the initial deviation of the shells from the perfect toroidal form is denoted by $\bar{w}$ and is taken to be

$$\bar{w} = \bar{\xi} h \sin(\pi x/l)\sin(ny/r_y) \tag{5}$$

where here also, the imperfection $\bar{\xi}$ is measured relative to the shell thickness.

The equilibrium equation obtained from the Koiter analysis, valid in the initial post-buckling regime, is of the form

$$\left(1-\frac{\lambda}{\lambda_c}\right)\xi + a\xi^2 + b\xi^3 + \ldots = \frac{\lambda}{\lambda_c}\bar{\xi} + \text{order } \xi\bar{\xi} + \ldots \tag{6}$$

where λ/λ_c is the ratio of the applied load λ to the classical buckling load λ_c. The derivation of this equation and the calculation of the coefficients a and b are given in the Appendix.

Each of the structure–load combinations considered in this paper is of the "cubic type"; that is, a is identically zero and the initial post-buckling behavior is determined by the term $b\xi^3$ in the equilibrium equation. Thus the governing equation is

$$\left(1-\frac{\lambda}{\lambda_c}\right)\xi+b\xi^3=\frac{\lambda}{\lambda_c}\bar{\xi}. \tag{7}$$

This equation is asymptotically valid for small ξ and $\bar{\xi}$.

The load–deflection behavior of the cubic structure is depicted in the two plots of Fig. 3. The perfect structure, $\bar{\xi}=0$, suffers no deflection in the ξ mode prior to buckling.

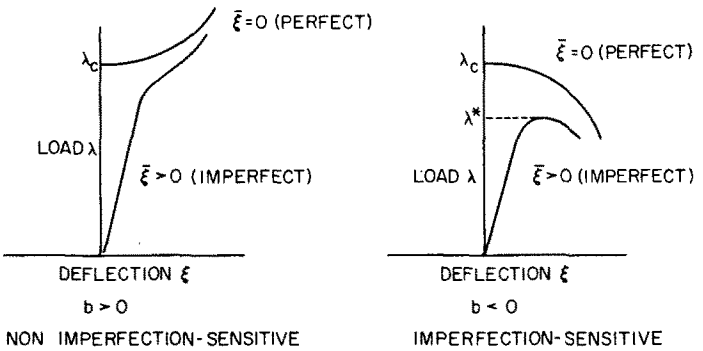

FIG. 3. Load–deflection behavior of cubic structure.

At $\lambda=\lambda_c$ bifurcation from the prebuckling state occurs. If $b>0$ the applied λ *increases* with increasing deflection ξ; while if $b<0$ the equilibrium curve of λ vs. ξ *falls* in the initial post-buckling region. The effect of an initial imperfection on the load–deflection behavior is also shown in these two plots. Only in the latter case, namely $b<0$, is the cubic structure *imperfection-sensitive* in the sense that imperfections result in reduced values of the maximum load the structure can support. An expression relating the buckling load (maximum load) λ^* of the imperfect structure to the imperfection magnitude for the case $b<0$ is easily found from equation (7) in conjunction with the condition $d\lambda/d\xi=0$. This equation is

$$\left(1-\frac{\lambda^*}{\lambda_c}\right)^{\frac{3}{2}}=\frac{3\sqrt{3}}{2}(\sqrt{-b})|\bar{\xi}|\frac{\lambda^*}{\lambda_c}.$$

The plot of λ^*/λ_c vs. $(\sqrt{-b})|\bar{\xi}|$ is given in Fig. 4. If $\sqrt{-b}$ is of order unity, imperfections which are small relative to the shell thickness (i.e., $\bar{\xi}$ a small fraction of unity) will result in large reductions of the buckling load.

The results of the b calculation for the three loading cases are presented and discussed in the next three sections; and as we have mentioned, the details of the calculations are left for the Appendix.

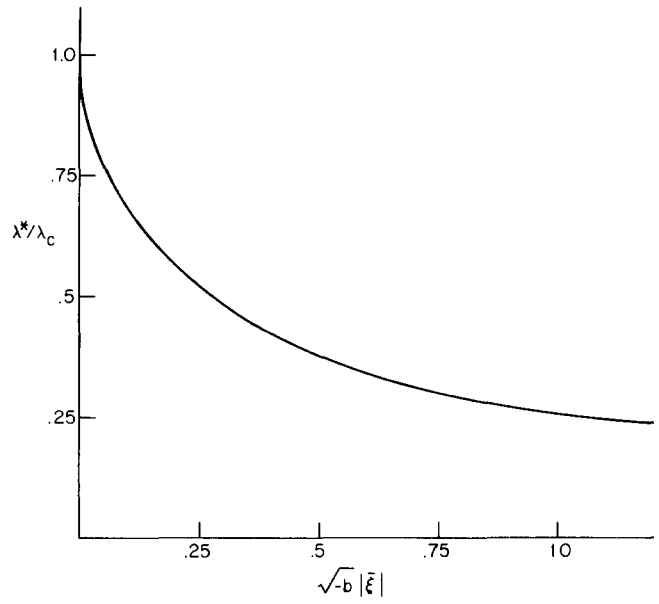

FIG. 4. Buckling load vs. imperfection relation.

TOROIDAL SEGMENT SUBJECT TO LATERAL PRESSURE

The prebuckling state of stress of a perfect, shallow toroidal segment subject to lateral pressure p is uniform, except in a narrow region near the ends of the shell, and is given by

$$\lambda N_x^0 = 0 \quad \text{and} \quad \lambda N_y^0 = -pr_y. \tag{8}$$

Results from the classical buckling analysis have been referred to in the introduction and

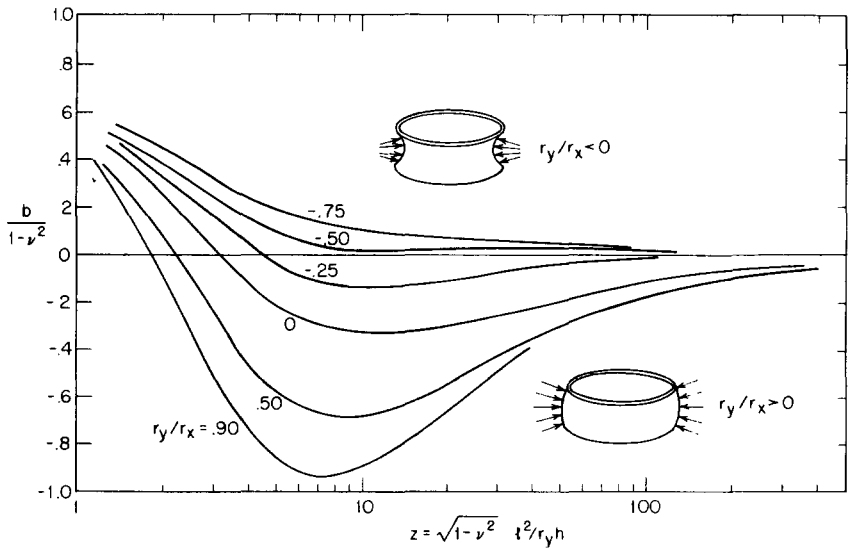

FIG. 5. Initial post-buckling coefficient for lateral pressure case.

are shown in Fig. 2. This is a plot of the buckling parameter $K = pr_y l^2/\pi^2 D$ as a function of $z = (1-\nu^2)^{\frac{1}{2}} l^2/r_y h$ for several values of r_y/r_x.

Figure 5 contains plots of $b/(1-\nu^2)$, again, as a function of z for several values of r_y/r_x. The bowed-out segments, $r_y/r_x > 0$, are imperfection-sensitive (i.e. $b < 0$) over a major part of the range of z. The more the toroidal shell is bowed-out the more negative is b and, thus, the more sensitive the structure to imperfections. There is a significant range, even for the cylindrical shell ($r_y/r_x = 0$), for which $\sqrt{-b}$ is of order unity, and small imperfections relative to the shell thickness will, therefore, result in significant reductions in the buckling pressure. For configurations which are sufficiently bowed-in b is actually positive, although quite small for sufficiently large z, over the entire range of z. Interpretation of the curves for $z < 10$ must be viewed as qualitative since then the details of the prebuckling deformation will quite likely become important. The bowed-out shell has a higher imperfection-sensitivity associated with its considerably higher classical buckling load.

The initial slope of the generalized load–deflection curve of the perfect shell can also be determined from the initial post-buckling analysis. This calculation is given in the Appendix. The resulting relation of pressure to average lateral deflection is

$$\frac{w_{ave}}{w_{oc}} = \frac{\lambda}{\lambda_c} + \frac{1}{\kappa}\left(\frac{\lambda}{\lambda_c} - 1\right) \tag{9}$$

where w_{ave} is the average normal displacement of the shell and w_{oc} is the prebuckling normal displacement at the critical pressure. The coefficient κ, also calculated in the Appendix, is plotted in Fig. 6 as a function of z for several values of r_y/r_x.

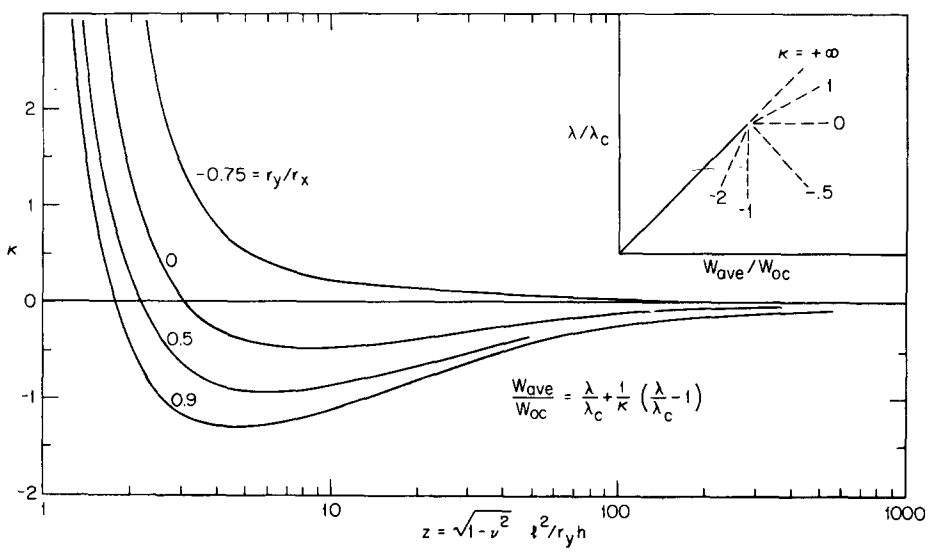

FIG. 6. Initial post-buckling pressure–lateral deflection relation.

The results for the lateral pressure buckling of a cylindrical shell ($r_y/r_x = 0$) are in agreement with results obtained previously by Budiansky and Amazigo [4]. The method employed here is the same as that used by these authors. Koiter [5] has determined the initial post-buckling behavior of narrow cylindrical panels under axial compression.

Like the toroidal shells considered here the narrow panel has a unique buckling mode and its initial post-buckling behavior is determined by the coefficient b of the cubic term in equation (7). Koiter finds that depending on the narrowness of the panel the post-buckling behavior can correspond to either an initially rising or falling load–deflection curve.

TOROIDAL SEGMENTS SUBJECT TO EXTERNAL PRESSURE

In this case there is a prebuckling axial compressive stress in addition to the circumferential stress according to

$$\lambda N_x^0 = -\tfrac{1}{2}pr_y \quad \text{and} \quad \lambda N_y^0 = -pr_y(1-r_y/2r_x). \tag{10}$$

The results of the classical buckling analysis are shown in Fig. 7. The trends are similar to the lateral pressure case although it is noted that the discrepancy between the buckling pressures of the bowed-in and bowed-out shells is emphasized even more.

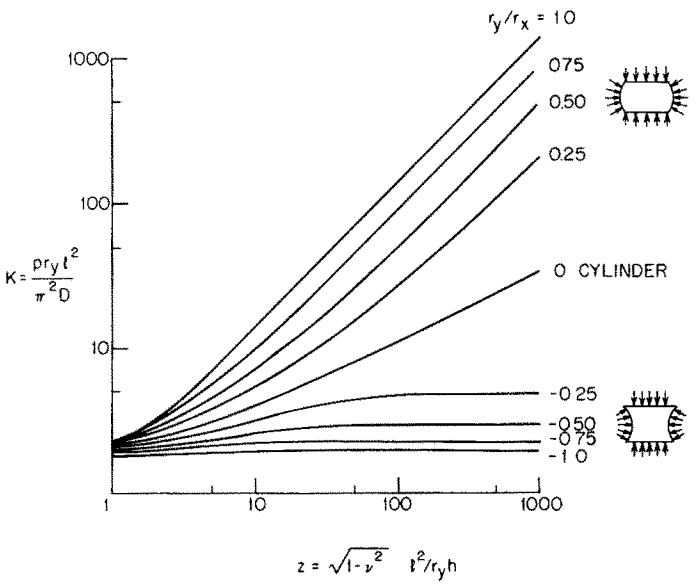

FIG. 7. Classical buckling of toroidal segments under external hydrostatic pressure.

Plots of $b/(1-\nu^2)$ vs. z for different values of r_y/r_x are shown in Fig. 8. As would be expected the shells are more imperfection-sensitive than in the previous case.

When $r_y/r_x = 1$ the shell is locally spherical at each point on its surface and the prebuckling stresses are exactly those corresponding to a complete spherical shell of similar radius and thickness, namely $N_x = N_y = -\frac{1}{2}pr$. The classical buckling pressure of the $r_y/r_x = 1$ case for large z is also that for a complete spherical shell

$$p = \frac{2}{\sqrt{[3(1-\nu^2)]}} E\left(\frac{h}{r}\right)^2.$$

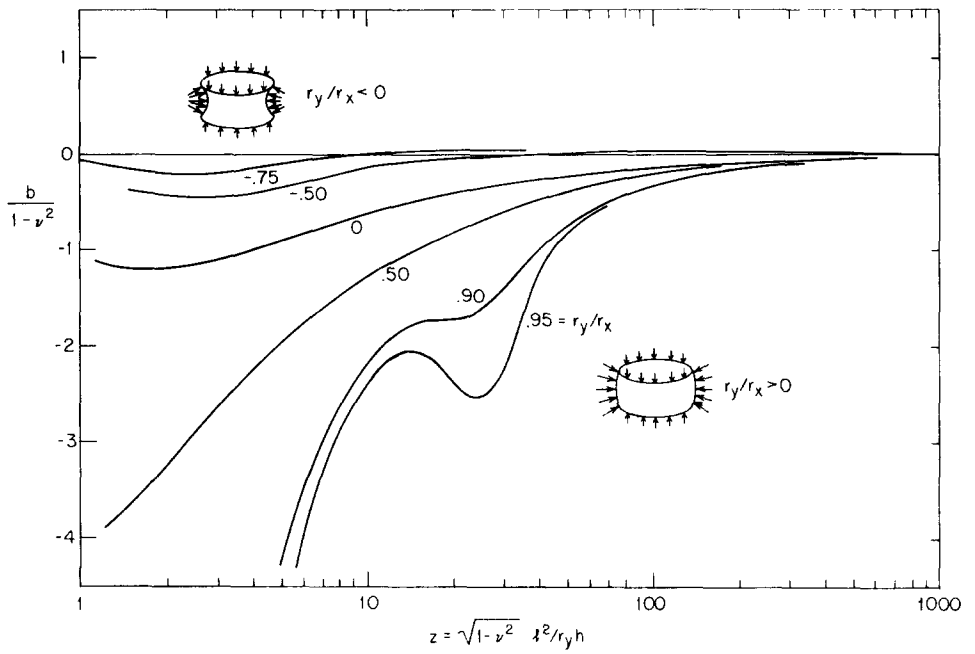

FIG. 8. Initial post-buckling coefficient for external pressure case.

Furthermore, when $r_y/r_x = 1$, there is not a unique buckling mode, but a large number of buckling modes associated with the classical buckling pressure and the analysis employed in this paper is no longer valid. The multimode post-buckling behavior of a shallow section of a complete spherical shell has been studied in [6]. The spherical shell is a "quadratic type" structure and the buckling load–imperfection relation for small imperfections $\bar{\xi}$ is of the form

$$1-\lambda/\lambda_c \approx (a\bar{\xi})^{\frac{1}{2}}$$

while the analogous relation for a "cubic" structure for small $\bar{\xi}$ is

$$1-\lambda/\lambda_c \approx [(\sqrt{\ }-b)\bar{\xi}]^{\frac{1}{3}}$$

The transition from the cubic type structure, $r_y/r_x < 1$, to the inherently more imperfection-sensitive quadratic character is reflected in the plots of b vs. z for values of r_y/r_x near unity.

The initial post-buckling behavior of externally pressurized cylindrical shells has also been studied by Budiansky and Amazigo and their results coincide with the $r_y/r_x = 0$ calculations presented here.

TOROIDAL SEGMENTS SUBJECT TO AXIAL TENSION

The prebuckling state of stress in the perfect toroidal shell resulting from an applied axial stress resultant N^0 is

$$\lambda N_x^0 = N^0, \qquad \lambda N_y^0 = -N^0 r_y/r_x \tag{11}$$

and a compressive circumferential stress will be induced only if $r_y/r_x > 0$. In other words, buckling in tension occurs only for the bowed-out shells. The results of the linear buckling analysis are given in Fig. 9 where, now, the buckling parameter is $K = N^0 l^2/\pi^2 D$.

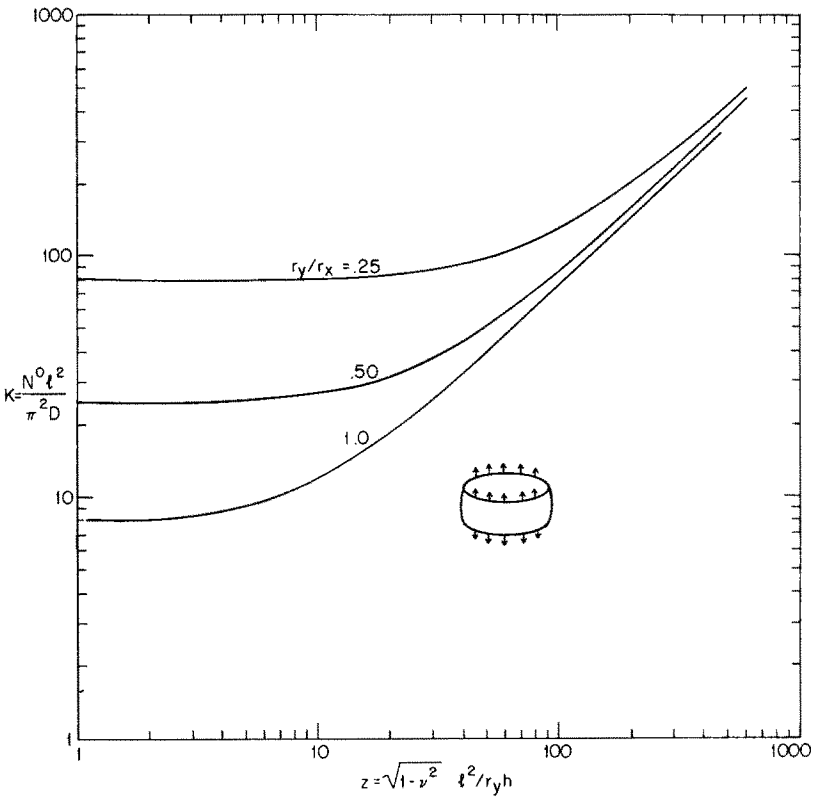

FIG. 9. Classical buckling of bowed-out toroidal segments under axial tension.

The b plots, analogous to those of Figs. 5 and 8, are presented in Fig. 10. If $r_y/r_x < \frac{1}{2}$ the toroidal segments appear to be relatively insensitive to imperfections. For values of the length parameter less than a certain value, depending on r_y/r_x, b is positive and the load increases in the initial post-buckling region.

Figure 11 gives plots of κ which appears in the load–elongation relation of the perfect shell

$$\frac{\varepsilon}{\varepsilon_{oc}} = \frac{\lambda}{\lambda_c} + \frac{1}{\kappa}\left(\frac{\lambda}{\lambda_c} - 1\right) \tag{12}$$

where ε is the axial elongation and ε_{oc} is the prebuckling axial elongation at the critical load. Depending on the value of r_y/r_x and z, the slope of the initial post-buckling load elongation curve can be either almost that of the prebuckling curve or sharply falling. These calculations are given in the Appendix.

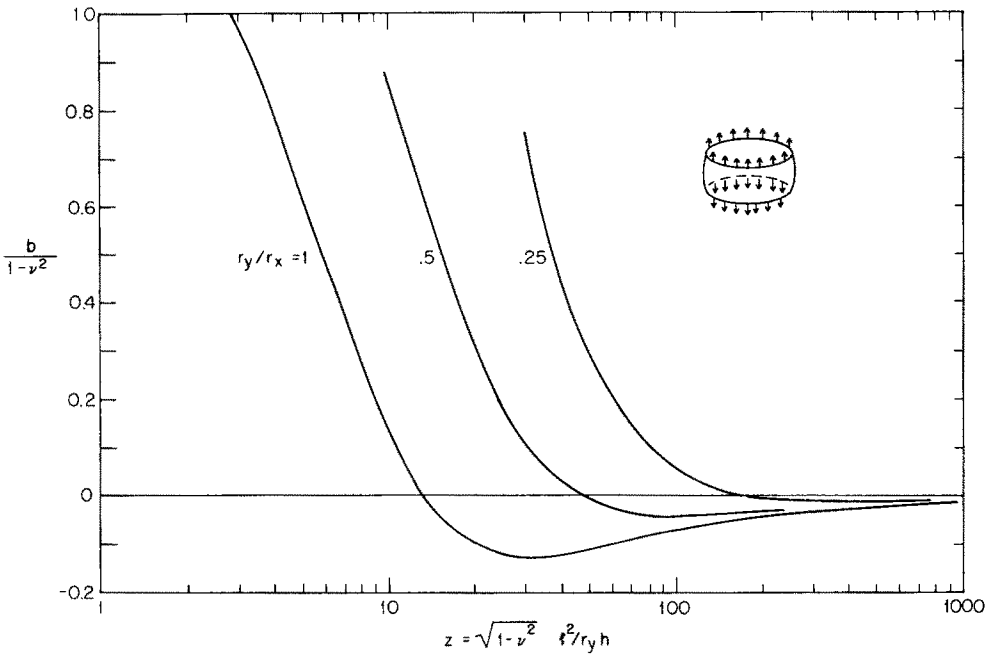

FIG. 10. Initial post-buckling coefficient for buckling under axial tension.

Yao [7] compared experimentally obtained buckling loads of axially loaded, truncated hemispheres with predictions based on a linear buckling analysis. The results presented

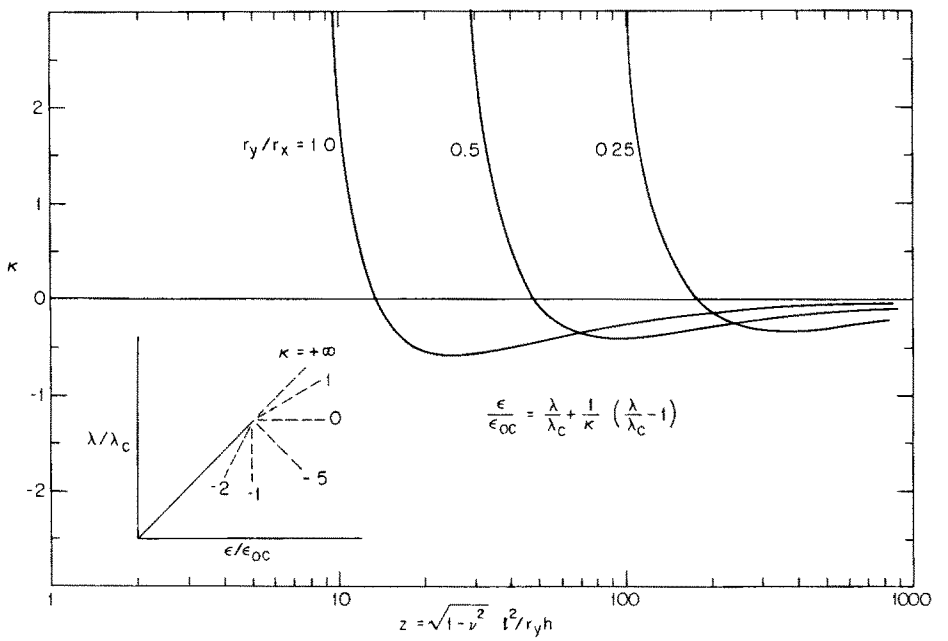

FIG. 11. Load–elongation relation in initial post-buckling of toroidal segments subject to axial tension [$\nu = \frac{1}{3}$].

in this section for segments of spheres, $r_y/r_x = 1$, are not directly applicable since both Yao's calculations and the tests correspond to clamped end conditions. On the other hand, qualitative agreement should be expected with respect to the degree of imperfection-sensitivity of clamped and simply supported shells. The test specimens were sufficiently short (i.e. l/r_x sufficiently small) to justify, if only approximately, the shallowness assumption made in the present analysis. The test buckling loads ranged from one third to slightly over one half the classical buckling loads with the length parameters falling in the range $50 < z < 300$. It is interesting to note that the range of the z's of the test specimens falls within the imperfection-sensitive range predicted by the present analysis.

REFERENCES

[1a] W. T. KOITER, *Over de Stabiliteit van het Elastisch Evenwicht* (with a summary in English). Thesis, Delft, H. J. Paris, Amsterdam.

[1b] W. T. KOITER, Elastic Stability and post-buckling behavior. Proc. Symp. on *Nonlinear Problems*, edited by R. E. Langer, p. 257. Univ. of Wisc. Press (1963).

[2] M. STEIN and J. A. MCELMAN, Buckling of segments of toroidal shells. *AIAA Jnl* **3**, 1704 (1965).

[3] B. O. ALMROTH, Influence of edge conditions on the stability of axially compressed cylindrical shells. *AIAA Jnl* **4**, 134 (1966).

[4] B. BUDIANSKY and J. AMAZIGO, Private communication on initial post-buckling behavior of externally pressurized cylindrical shells. To be published.

[5] W. T. KOITER, Buckling and post-buckling behavior of a cylindrical panel under axial compression. Report S. 476, Nat. Aero. Res. Inst., Amsterdam (1956).

[6] J. W. HUTCHINSON, Imperfection-sensitivity of externally pressurized spherical shells. To be published in *J. appl. Mech.*

[7] J. C. YAO, Buckling of a truncated hemisphere under axial tension. *AIAA Jnl* **1**, 2316 (1963).

[8] B. BUDIANSKY and J. HUTCHINSON, Dynamic buckling of imperfection-sensitive structures. *Proc. 11th Int. Congr. Applied Mech.* (1964). Springer. To be published.

APPENDIX: INITIAL POST-BUCKLING CALCULATIONS

Donnell-type nonlinear shell equations

The *membrane strains* ε_x, ε_y and ε_{xy} of Donnell-type theory are related to the normal and tangential displacements to the shell middle surface w, u, v by

$$\begin{aligned} \varepsilon_x &= u_{,x} + w/r_x + \tfrac{1}{2}w_{,x}^2 + \bar{w}_{,x}w_{,x} \\ \varepsilon_y &= v_{,y} + w/r_y + \tfrac{1}{2}w_{,y}^2 + \bar{w}_{,y}w_{,y} \end{aligned} \tag{13}$$

and

$$2\varepsilon_{xy} = v_{,x} + u_{,y} + w_{,x}w_{,y} + \bar{w}_{,x}w_{,y} + w_{,x}\bar{w}_{,y}$$

where $\bar{w}$ is the initial normal deflection of the shell middle surface from the perfect toroidal segment with radii r_x and r_y. The *bending strain–displacement relations* are linear: $k_x = -w_{,xx}$, $k_y = -w_{,yy}$ and $k_{xy} = -w_{,xy}$. The *stress–strain relations* are also linear: $E\varepsilon_x = N_x - \nu N_y$, $M_x = D(k_x + \nu k_y)$, etc.

Equations of equilibrium can be formulated in terms of a variational principle of virtual

work. For Donnell theory the statement of this principle is

$$\int_S (N_x\delta\varepsilon_x + N_y\delta\varepsilon_y + 2N_{xy}\delta\varepsilon_{xy} + M_x\delta k_x + M_y\delta k_y + 2M_{xy}\delta k_{xy})\,\mathrm{d}S + \int_S \lambda p^0\delta w\,\mathrm{d}S - \int_C \lambda N^0\delta u\,\mathrm{d}s = 0 \tag{14}$$

where λp^0 is the applied pressure, λN^0 is the stress resultant applied at the ends of the shell and $\delta\varepsilon_x = \delta u_{,x} + \delta w/r_x + w_{,x}\delta w_{,x} + \bar{w}_{,x}\delta w_{,x}$, $\delta k_x = -\delta w_{,xx}$, etc. The scalar load parameter λ has been introduced to emphasize that for each loading combination considered in this paper the axial load and lateral pressure are fixed in a definite ratio. Thus, N^0 and p^0 are assumed fixed in a manner appropriate to the particular loading combination. The differential equations associated with this variational principle are the three equilibrium equations, which when expressed in terms of the three displacements u, v, w, provide the set of Donnell-type equations governing the deformation of the shell. *Boundary conditions* in this analysis are taken to be v (the circumferential displacement) $= w = M_x = 0$ and $N_x = \lambda N^0$ at the ends of the shell, $x = 0, l$.

The *prebuckling stresses* in the perfect shell for a given lateral pressure loading λp^0 and applied axial stress λN^0 are uniform, except for deviations in a narrow region near the ends of the shell which will be neglected in this analysis. The nonzero prebuckling stresses and deformations are

$$\lambda N_x^0 = \lambda N^0, \qquad \lambda N_y^0 = -\lambda(p^0 r_y + N^0 r_y/r_x) \tag{15}$$

$$\lambda w^0 \doteq -\frac{\lambda r_y}{Eh}[N^0(r_y/r_x + \nu) + p^0 r_y] \tag{16}$$

and

$$\lambda u_{,x}^0 = \frac{\lambda}{Eh}\{N^0[(r_y/r_x)^2 + 2\nu r_y/r_x + 1] + p^0 r_y(r_y/r_x + \nu)\}$$

Initial post-buckling analysis for unique mode buckling

The notation and development of Koiter's general theory displayed here are taken from [8]. Only the outline and essential results of the theory will be given. The reader is referred to [8] or Koiter's own work [1] for omitted details and points of rigor which will not be re-established here. For brevity, the *stress*, *strain* and *displacement* fields are denoted by σ, ε and u, respectively.* The magnitude of the applied load system is taken to be directly proportional to the load parameter λ.

The *strain–displacement relations* of the perfect shell are written symbolically as

$$\varepsilon = L_1(u) + \tfrac{1}{2}L_2(u) \tag{17}$$

where L_1 and L_2 are, then, homogeneous functionals which are linear and quadratic, respectively, in u. In the presence of an initial deflection of the unloaded structure $\bar{u}$ the strain resulting from an additional displacement u is

$$\varepsilon = L_1(u) + \tfrac{1}{2}L_2(u) + L_{11}(u, \bar{u}) \tag{18}$$

* In the general development u is a generalized expression for the displacements. It should not be confused with the axial displacement in the Donnell theory which bears the same symbol.

where $L_{11}(u, \bar{u}) = L_{11}(\bar{u}, u)$ is the bilinear, homogeneous functional of u and $\bar{u}$ which appears in the identity.

$$L_2(u+\bar{u}) = L_2(u)+2L_{11}(u, \bar{u})+L_2(\bar{u}).$$

The *stress–strain relations* are linear and are denoted by

$$\sigma = H_1(\varepsilon) \tag{19}$$

where H_1 is a homogeneous, linear functional.

Equations of equilibrium are formulated via the principle of virtual work. In compact form this principle (equation (14) for Donnell theory) is written as

$$\{\sigma, \delta\varepsilon\} - \lambda B_1(\delta u) = 0 \tag{20}$$

where $\{\sigma, \delta\varepsilon\}$ is the internal virtual work of the stress field σ through the strain variation $\delta\varepsilon$ and $\lambda B_1(\delta u)$ is the external virtual work of the load system of intensity λ through the admissible displacement variation δu.

The prebuckling deformations of the perfect shells, equation (16), are linearly dependent on the applied load and are abbreviated as λu_0. Since the prebuckling strains are linearly dependent on the displacements, i.e. $L_2(u_0) = 0$, the prebuckling stresses, equation (15), are denoted by $\lambda\sigma^0$ and are related to λu_0 by $\sigma^0 = H_1[L_1(u_0)]$. To discover the eigenvalue λ_c and eigenmode u_c for *classical buckling* we set

$$u = \lambda_c u_0 + u_c$$

in the field equations and retain only the linear terms in the buckling mode u_c. The resulting variational equation is, in the compact notation,

$$\lambda_c\{\sigma_0, L_{11}(u_c, \delta u)\} + \{s_c, L_1(\delta u)\} = 0 \tag{21}$$

where $s_c = H_1[L_1(u_c)]$. When this statement is translated into Donnell notation the differential equations associated with this variational equation are the linear buckling equations which, when written in terms of a stress function and the normal displacement in the usual manner, become equations (1) and (2).

As previously mentioned, each structure–loading combination investigated in this paper has a unique buckling mode associated with the classical buckling load. To study the *initial post-buckling behavior* one writes the total displacement, quite generally, as

$$u = \lambda u_0 + \xi u_c + \tilde{u} \tag{22}$$

where u_c is now considered normalized in magnitude in a definite way. The displacement $\tilde{u}$ is taken to be orthogonal to u_c in the sense

$$\{\sigma_0, L_{11}(u_c, \tilde{u})\} = 0 \tag{23}$$

When a structure is imperfection-sensitive, imperfections in the form of the buckling mode are most critical. In this study the imperfection is taken as

$$\bar{u} = \bar{\xi} u_c \tag{24}$$

The initial post-buckling analysis provides an algebraic equilibrium equation relating ξ, $\bar{\xi}$ and the load parameter λ. This equation is a representation which is uniformly valid

for small ξ and $\bar{\xi}$. To obtain this equation one writes

$$\tilde{u} = \xi^2 u_2 + \xi^3 u_3 + \ldots + \bar{\xi}[\xi u_{11} + \xi^2 u_{21} + \ldots] + \ldots \tag{25}$$

and then u as given by (22), with the aid of equations (17)–(19), is substituted into the variational equilibrium equation. The requirement that equation (20) be satisfied for the variation $\delta u = u_c \delta\xi$ gives the scalar equation relating λ to ξ and $\bar{\xi}$

$$\begin{aligned} &-\xi(\lambda_c - \lambda)\{\sigma_0, L_2(u_c)\} + \tfrac{3}{2}\xi^2\{s_c, L_2(u_c)\} \\ &\quad + \xi^3[2\{s_c, L_{11}(u_c, u_2)\} + \{s_2, L_2(u_c)\} + \tfrac{1}{2}\{H_1(L_2(u_c)), L_2(u_c)\}] \\ &\quad + O(\xi^4) + \ldots = -\xi\lambda\{\sigma_0, L_2(u_c)\} + O(\xi\bar{\xi}, \bar{\xi}^2) + \ldots \end{aligned} \tag{26}$$

where $s_2 = H_1[L_1(u_2)]$. For all variations δu orthogonal to u_c, equation (20) provides the variational equation necessary for determining u_2

$$\begin{aligned} &\lambda_c\{\sigma_0, L_{11}(u_2, \delta u)\} + \{s_2, L_1(\delta u)\} = \\ &\qquad -\{s_c, L_{11}(u_c, \delta u)\} - \tfrac{1}{2}\{H_1[L_2(u_c)], L_1(\delta u)\}. \end{aligned} \tag{27}$$

Equation (26) can be written in the form of equation (6) given in the body of the report, i.e.

$$\left(1 - \frac{\lambda}{\lambda_c}\right)\xi + a\xi^2 + b\xi^3 + \ldots = \frac{\lambda}{\lambda_c}\bar{\xi} + \ldots \tag{6}$$

where the coefficients a and b are

$$a = \frac{\frac{3}{2}\{s_c, L_2(u_c)\}}{-\lambda_c\{\sigma_0, L_2(u_c)\}} \tag{28}$$

and

$$b = \frac{2\{s_c, L_{11}(u_c, u_2)\} + \{s_2, L_2(u_c)\} + \frac{1}{2}\{H_1[L_2(u_c)], L_2(u_c)\}}{-\lambda_c\{\sigma_0, L_2(u_c)\}} \tag{29}$$

Calculation of the b coefficient for toroidal shell segments

The buckling mode (4) is such that the λ vs. ξ relation of the perfect toroidal shell can depend only on the magnitude of ξ and not on its sign and, thus, a must be zero. This can be verified directly by noting that

$$\begin{aligned} \{s_c, L_2(u_c)\} &= \int_S (f_{c,yy} w_{c,x}^2 + f_{c,xx} w_{c,y}^2 - 2 f_{c,xy} w_{c,x} w_{c,y})\, dS \\ &= 0 \end{aligned}$$

where, consistent with equation (4),

$$\begin{aligned} w_c &= h \sin(\pi x/l) \sin(ny/r_y) \\ f_c &= -\frac{Eh^2 l^2 A}{\pi^2 r_y} \sin(\pi x/l) \sin(ny/r_y) \end{aligned} \tag{30}$$

and

$$A = \left[\frac{1+\bar{n}^2 r_y/r_x}{(1+\bar{n}^2)^2}\right].$$

The initial post-buckling behavior, then, is determined by b as long as this coefficient does not also vanish. Evaluation of b necessitates solving for u_2. A straightforward translation of the variational equation (27) into Donnell notation followed by the usual calculus of variations procedure leads to three simultaneous partial differential equations for u_2, v_2 and w_2. These equations are

$$\begin{aligned} D\nabla^4 w_2 + \frac{1}{r_x}N_x^{(2)} + \frac{1}{r_y}N_y^{(2)} - \lambda_c N_x^0 w_{2,xx} - \lambda_c N_y^0 w_{2,yy} \\ = f_{c,yy}w_{c,xx} + f_{c,xx}w_{c,yy} - 2f_{c,xy}w_{c,xy} \\ -\frac{1}{2}\frac{Eh}{1-\nu^2}\left[\frac{1}{r_x}(w_{c,x}^2 + \nu w_{c,y}^2) + \frac{1}{r_y}(w_{c,y}^2 + \nu w_{c,x}^2)\right] \end{aligned}$$

$$N_{x,x}^{(2)} + N_{xy,y}^{(2)} = -\frac{1}{2}\frac{Eh}{1-\nu^2}[(w_{c,x}^2 + \nu w_{c,y}^2)_{,x} + (1-\nu)(w_{c,x}w_{c,y})_{,y}]$$

$$N_{y,y}^{(2)} + N_{xy,x}^{(2)} = -\frac{1}{2}\frac{Eh}{1-\nu^2}[(w_{c,y}^2 + \nu w_{c,x}^2)_{,y} + (1-\nu)(w_{c,x}w_{c,y})_{,x}]$$

with the boundary conditions $w_2 = w_{2,xx} = v_2 = 0$ and $N_x^{(2)} + \frac{1}{2}[Eh/(1-\nu^2)]\cdot[w_{c,x}^2 + \nu w_{c,y}^2] = 0$ at $x = 0, l$, where $N_x^{(2)} = (Eh/1-\nu^2)[u_{2,x} + w_2/r_x + \nu(v_{2,y} + w_2/r_y)]$, etc.

These equations are reduced to a much more manageable form if the stress function f_2 is introduced according to

$$N_x^{(2)} = f_{2,yy} - \frac{1}{2}\frac{Eh}{1-\nu^2}(w_{c,x}^2 + \nu w_{c,y}^2)$$

$$N_y^{(2)} = f_{2,xx} - \frac{1}{2}\frac{Eh}{1-\nu^2}(w_{c,y}^2 + \nu w_{c,x}^2)$$

$$N_{xy}^{(2)} = -f_{2,xy} - \frac{1}{2}\frac{Eh}{1+\nu}w_{c,x}w_{c,y}.$$

Then the equations for w_2 and f_2 become

$$\begin{aligned} D\nabla^4 w_2 + \frac{1}{r_y}f_{2,xx} + \frac{1}{r_x}f_{2,yy} - \lambda_c N_x^0 w_{2,xx} - \lambda_c N_y^0 w_{2,yy} \\ = f_{c,yy}w_{c,xx} + f_{c,xx}w_{c,yy} - 2f_{c,xy}w_{c,xy}. \end{aligned} \tag{31}$$

and secondly, the compatibility equation

$$\frac{1}{Eh}\nabla^4 f_2 - \frac{1}{r_y}w_{2,xx} - \frac{1}{r_x}w_{2,yy} = w_{c,xy}^2 - w_{c,xx}w_{c,yy} \tag{32}$$

and the boundary conditions reduce to

$$w_2 = w_{2,xx} = f_{2,xx} = f_2 = 0 \quad \text{at} \quad x = 0, l.$$

A stress function has been introduced and, thus, a further condition is that the tangential displacements be single valued over a complete circuit of the shell. For v_2 this condition is equivalent to

$$\int_0^{2\pi r_y} \left[\frac{1}{Eh}(f_{2,xx}-\nu f_{2,yy})-\frac{1}{2}w_{c,y}^2-\frac{w_2}{r_y}\right] dy = 0. \tag{33}$$

The right hand sides of equations (31) and (32) are respectively,

$$-\frac{Eh^3A(\bar{n}\pi/l)^2}{r_y}[\cos(2\pi x/l)+\cos(2ny/r_y)] \quad \text{and} \quad \tfrac{1}{2}h^2\bar{n}^2(\pi/l)^4[\cos(2\pi x/l)+\cos(2ny/r_y)].$$

The solution to equations (31) and (32) can be written in the separated form

$$w_2 = \sum_{i=1,3,5\ldots}^{\infty} \alpha_i \sin(i\pi x/l)+\cos(2ny/r_y) \sum_{i=1,3,5\ldots}^{\infty} \gamma_i \sin(i\pi x/l) \tag{34}$$

and

$$f_2 = \sum \beta_i \sin(i\pi x/l)+\cos(2ny/r_y)\sum \delta_i \sin(i\pi x/l) \tag{35}$$

and the coefficients of these series can be determined with the Galerkin procedure. One finds

$$\begin{aligned}
\alpha_i &= \pi(1-\nu^2)^{\frac{1}{2}}\bar{n}^2h\bar{\alpha}_i = \pi(1-\nu^2)^{\frac{1}{2}}\bar{n}^2h(Ai^2+\tfrac{1}{2})/Q_i \\
\beta_i &= \pi\bar{n}^2Eh^3\bar{\beta}_i = \pi\bar{n}^2Eh^3(\pi^2i^2/24z+\lambda_c\bar{N}_x^0/2-Az/\pi^2)/Q_i \\
\gamma_i &= 4\pi(1-\nu^2)^{\frac{1}{2}}\bar{n}^2h\bar{\gamma}_i = 4\pi(1-\nu^2)^{\frac{1}{2}}\bar{n}^2h[A(i^2+4\bar{n}^2)^2+i^2/2+2\bar{n}^2r_y/r_x]/H_i \\
\delta_i &= 4\pi\bar{n}^2Eh^3\bar{\delta}_i = 4\pi\bar{n}^2Eh^3[\pi^2(i^2+4\bar{n}^2)^2/24z+\lambda_c\bar{N}_x^0i^2/2 \\
&\qquad +2\lambda_c\bar{N}_y^0\bar{n}^2-z(i^2+4\bar{n}^2r_y/r_x)A/\pi^2]/H_i \\
&\quad i = 1,3,5\ldots
\end{aligned}$$

with

$$\begin{aligned}
Q_i &= i(i^2-4)(\pi^4i^4/12z+\lambda_c\bar{N}_x^0\pi^2i^2+z)/4 \\
H_i &= i[\pi^4(i^2+4\bar{n}^2)^4/12z+\lambda_c\bar{N}_x^0\pi^2i^2(i^2+4\bar{n}^2)^2+\lambda_c\bar{N}_y^04\pi^2\bar{n}^2(i^2+4\bar{n}^2)^2 \\
&\qquad +z(i^2+4\bar{n}^2r_y/r_x)^2]
\end{aligned}$$

and where $\lambda_c\bar{N}_x^0 = \lambda_c(1-\nu^2)^{\frac{1}{2}}r_yN_x^0/Eh^2$ and $\lambda_c\bar{N}_y^0 = \lambda_c(1-\nu^2)^{\frac{1}{2}}r_yN_y^0/Eh^2$.

That this solution satisfies the single valued conditions can be verified by direct substitution into equation (33), for example. Alternatively one notes immediately that the y dependent terms in (34) and (35) satisfy equation (33). Then one can recognize that equation (32), for the y independent part of the solution, when integrated twice with respect to x in conjunction with the boundary conditions is precisely condition (33). Similarly one can show that u_2 is single valued.

Now, b can be calculated using equation (29) if it is noted that

$$-\lambda_c\{\sigma_0, L_2(u_c)\} = -\lambda_c \int_S (N_x^0 w_{c,x}^2 + N_y^0 w_{c,y}^2)\, dS$$

$$\{s_c, L_{11}(u_c, u_2)\} = \int_S [f_{c,yy} w_{c,x} w_{2,x} + f_{c,xx} w_{c,y} w_{2,y} - f_{c,xy}(w_{c,x} w_{2,y} + w_{c,y} w_{2,x})]\, dS$$

and

$$\{s_2, L_2(u_c)\} + \tfrac{1}{2}\{H_1[L_2(u_c)], L_2(u_c)\} = \int_S (f_{2,yy} w_{c,x}^2 + f_{2,xx} w_{c,y}^2 - 2 f_{2,xy} w_{c,x} w_{c,y})\, dS.$$

The result of this calculation is

$$b = \frac{-8(1-\nu^2)\bar{n}^4}{\lambda_c(\bar{N}_x^0 + \bar{N}_y^0 \bar{n}^2)}\left[\left(\sum \bar{\beta}_i \frac{i}{(i^2-4)} + 2\sum \bar{\delta}_i \frac{1}{i}\right)\pi^2/z - 2A\left(\sum \bar{\alpha}_i \frac{i}{(i^2-4)} + 2\sum \bar{\gamma}_i \frac{1}{i}\right)\right]. \quad (36)$$

For the three loading cases presented in this paper the b calculations were made with the aid of a digital computer. The series in equation (36) were evaluated by taking a sufficiently large number of terms to insure that the truncation error was less than $\frac{1}{10}$ of one percent.

The generalized load–deflection relation for the lateral pressure case was calculated directly from the expression for the total normal displacement

$$w = \lambda w_0 + \xi w_c + \xi^2 w_2 + \ldots.$$

Since $\int w_c\, dS = 0$ and $\xi^2 = -(1-\lambda/\lambda_c)/b$, the initial post-buckling load–deflection relation between the average lateral deflection of the perfect shell and the lateral pressure is

$$\frac{w_{ave}}{w_{oc}} = \frac{\lambda}{\lambda_c} + \eta\left(1 - \frac{\lambda}{\lambda_c}\right) \quad (37)$$

where $w_{oc} = \lambda_c w_0$ is the prebuckling displacement at the critical pressure and

$$\eta = \frac{-1}{2\pi r_y l b w_{oc}} \int_S w_2\, dS.$$

This coefficient was calculated using a series representation, not given here, which was obtained from the expression for w_2, equation (34). It is more convenient to rewrite equation (37) in the form given in the body of the paper, namely,

$$\frac{w_{ave}}{w_{oc}} = \frac{\lambda}{\lambda_c} + \frac{1}{\kappa}\left(\frac{\lambda}{\lambda_c} - 1\right) \quad (9)$$

where $\kappa = -1/\eta$. Plots of κ as a function of z for several values of r_y/r_x are given in Fig. 6. Neglect of the distortion of the shell near its ends places the same limitation on the load–deflection relation and buckling load–imperfection relation as has been remarked on previously with regard to the classical buckling analysis.

In a similar fashion the axial load–elongation relation for the initial post-buckling regime of a perfect shell in axial tension can be calculated directly. The average elongation is

$$\varepsilon = \frac{1}{2\pi r} \int_S \left[\frac{1}{Eh}(N_x - \nu N_y) - \frac{w}{r_x} - \frac{1}{2} w_{,x}^2 \right] \mathrm{d}S.$$

The parameter in the load–deflection relation, equation (12), is again $\kappa = -1/\eta$ where now

$$\eta = \frac{-1}{2\pi r b \varepsilon_{oc}} \int_S \left[\frac{1}{Eh}(f_{2,yy} - \nu f_{2,xx}) - \frac{w_2}{r_x} - \frac{1}{2} w_{c,x}^2 \right] \mathrm{d}S$$

and ε_{oc} is the axial elongation at the onset of buckling. A series representation for η is obtained in a straightforward way. The results of the calculations are shown in Fig. 11 as plots of κ vs. z.

(*Received* 6 *January* 1966; *revised* 3 *March* 1966)

Résumé—Le comportement initial après flambement de segments d'enveloppe à double courbures, soumis à plusieurs conditions de charge, est déterminé en se basant sur la théorie générale de Koiter sur le comportement initial après flambement. Auparavant, l'on avait indiqué que les charges de flambage classiques associées à ces enveloppes dépendaient beaucoup des deux rayons de courbure et de leur grandeur relative. Dans cette étude, le comportement initial après flambement ainsi que l'imperfection-sensibilité y associée dépendent beaucoup des deux courbures également.

Zusammenfassung—Das anfängliche Benehmen nach dem Beulen von doppelt gebogenen Schalen-Segmenten die mehreren Belastungen unterworfen werden, wurden nach Koiters allgemeiner Theorie des Anfangsbenehmens bestimmt. Ehemals wurden die klassischen Beulungslasten als abhängig von zwei Krümmungs halbmessern und deren relativen Grössen dargestellt. In dieser Arbeit werden sowhl das Anfangsbenehmen wie auch die Fehler-Empfind-lichkeit als abhängig von den zwei Krümmungen gezeigt.

Абстракт—Первоначальное поведение сегментов оболочки двойной кривизны после быпугибания, допуская несколько условий нагрузки, определяется на основе общей теории Койтера (Koiter's) о первоначальном поведении после быпугибания. Ранее, классические нагрузки, вызывающие продольный изгиб, связанные с этими оболочками, оказались очень зависящими от двух радиусов кривизны и их относительной величины. Здесь, первоначальное поведение быпугибания, связанное с нарушением (дефектом) структуры чувствительности также показывает, что они очень зависят от той и другой кривизны.